Int J Adv Manuf Technol (2013) 65:333–342
DOI 10.1007/s00170-012-4172-6

ORIGINAL ARTICLE

Process simulation and optimization of laser tube bending

Yanjin Guan · Guiping Yuan · Sheng Sun · Guoqun Zhao

Received: 6 November 2008 / Accepted: 13 April 2012 / Published online: 5 May 2012

Abstract A 3D thermomechanical finite element analysis model for laser tube bending is developed based on the software MSC/Marc. The processes of single- and multi-scan are analyzed numerically. The gradient and development of the temperature between the laser scanning side and the nonscanning side leads to the changing complexity of the stress and strain. Consequently, the length of the laser scanning side becomes shorter than that of nonscanning side after cooling. The length difference between both sides makes the tube produce the bending angle. The relationship between the number of scans and the bending angle is about in direct ratio. The bending angle induced by the first irradiated time is largest. Meanwhile, the finite element simulation is integrated with the genetic algorithm. Aiming at different process demands, corresponding objective functions are established. Laser power, beam diameter, scanning velocity, and scanning wrap angle are regarded as design variables. Process optimizations of maximum angle bending and fixed angle bending after single laser scan are realized. Groups of optimized process parameters can be obtained according to different optimization objectives. The bending angle can approach to the maximum when the laser power, spot diameter, scanning velocity, and scanning wrap angle are 381.24 W, 3.37 mm, 16.34 mm/s, and 123.1°, respectively. When the laser power, spot diameter and scanning velocity are 426.12 W, 4.9 mm, 14.31 mm/s respectively, a fixed angle bending can be achieved.

Keywords Laser tube bending · FEM · Process simulation · Process optimization · Genetic algorithm

Y. Guan (✉) · S. Sun · G. Zhao
Key Laboratory for Liquid–Solid Structural Evolution and Processing of Materials Ministry of Education, Shandong University,
Jinan, China
e-mail: guan_yanjin@sdu.edu.cn

G. Yuan
Jining Vocational Technology College,
Jining 272000, China

1 Introduction

Laser bending is a noncontact method of 2D bending, 3D shaping, and precision alignment of metallic and nonmetallic components using laser energy [1–4]. Based on laser bending, sheets and tubes can be formed conveniently depending upon the non-uniform thermal stresses induced by laser heating.

Compared to laser bending of sheet metals, the laser tube bending is more complex because much more process parameters are involved. Meanwhile, the laser tube bending has a high demand on forming machine and tools. Thus, the forming process is hard to be controlled. Few researches involved laser tube bending. Nao and Li [5] investigated the developments of stress and strain during laser tube bending by means of a thermal–mechanical finite element transient analysis. A new analytical model [6] describing the bending angle was established. The model gives an analytical expression for the bending angle as a function of the energy (laser power, absorption, and scanning speed), geometric (tube diameter and wall thickness), and material properties (coefficient of thermal expansion, density, heat capacity, Young's modulus, and yield stress). Hsieh [7, 8] investigated the buckling mechanism of a thin metal tube with and without axial preloads during laser forming numerically and experimentally. Zhang [9] studied numerically different laser scanning schemes for tube bending without and with water cooling. Safdar [10] studied the effect of scanning direction on laser tube bending using finite element analysis.

Guglielmotti [11] studied bending of slotted tubes as well as enlarging of one tube end by means of a high power diode laser and found that high power diode lasers are very efficient laser sources for tube forming due to their large laser spot.

There are many influencing factors on laser tube forming, such as forming process parameters, material's properties, optic parameters, and geometrical parameters. Figure 1 gives factors of influence on laser tube bending. The melting point and yield strength are basic conditions to restrict to the forming process. For a given forming objective, material's properties and geometrical parameters of the tube are already decided. The aim of the laser tube bending is to acquire the desired bending deformation by means of the reasonable match of the process parameters.

As a high nonlinear forming process, the laser tube bending is hard to express the relationship of bending angle and process parameters by using a general formula. The finite element method is a powerful tool to study the laser bending of tubes. Using finite element method (FEM) process simulation, can be not only the final bending angle be acquired, but also kinds of fields, such as the stress, strain, displacement, and temperature fields, can be also obtained. The internal forming mechanisms can be revealed clearly. The FEM process simulation is an ideal researching method. Due to its complexity, a series of treatment techniques are necessary according to the characteristics of the laser tube bending. In this paper, the correlation between material's properties and temperature is considered, and a thermomechanical FEM model of the laser tube bending is established. Based on the FEM model, the process of laser tube bending is analyzed numerically.

To some extent, the FEM process simulation can realize the optimization of forming processes, too. However, it is hard to obtain the optimum process parameters only through FEM simulation. In practical work, it is very important to get the optimum process parameters. In this paper, the finite element method simulation process is integrated with the genetic algorithms and laser bending of tubes process is optimized based on different objection functions.

2 FEM modeling of process simulation

In the laser bending of tubes, the temperature and displacement fields affect each other. So it belongs to a typical coupled thermal–mechanical problem. A 3D coupled thermomechanical model for numerical simulation is necessary to reduce analytical errors significantly. Based on the thermal elastic–plastic finite element method, lots of technical treatments were done in this work. The coupled model was established to realize the simulation of the laser bending of tubes. The fields of thermal stress, temperature, and displacement can be obtained simultaneously by using the coupled model.

2.1 Selection of elements

In laser bending process, the temperature and deformation of the local heated zone were generated sharp variations during a very short time. Steep temperature and stress gradients occur. Higher precision can be acquired using brick element. Thus, brick elements are selected when the sheet is discretized during simulation.

The brick element is divided into full integral element and reduced integral element according to numerical

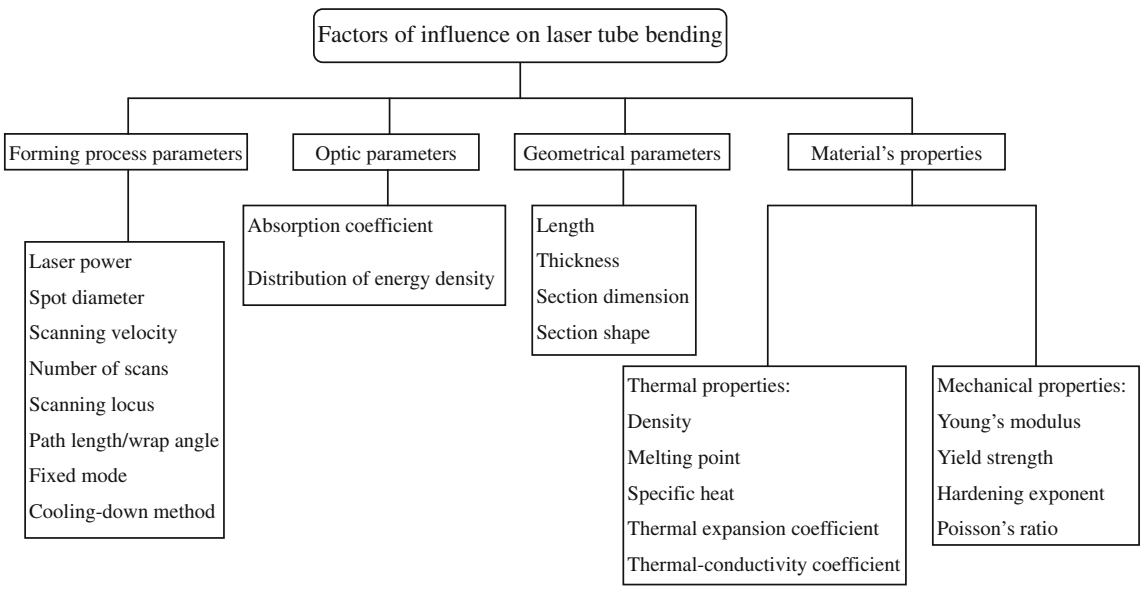

Fig. 1 Factors of influence on laser tube bending

integral way. For bending problem of the thin sheet, unreasonable results can be induced because of larger precision loss while selecting full integral element. Not only can be the calculation time of elements integration decreased using reduced integral way, but also analytical precision can be improved because of eliminating the influence of imperfect high-order term on results.

Meanwhile, a fine mesh is necessary around the laser beam path due to steep temperature and stress gradients in the heated zone. It is essential to have at least eight integration points in the thickness direction [12]. In order to cut the total number of elements in the simulation, a coarse mesh is used outside the current heating zone.

2.2 Treatment of the absorption coefficient

The absorption coefficient is up to absorptivity material versus laser and the surface appearance. When the laser beam irradiates the metal surface, the metal absorbs the light energy by means of the interaction of the photons, free electrons, and crystal lattice. Not only has the absorption coefficient of material something with physical characteristics, wavelength, light intensity, actuation duration, and material's electrical resistivity, but also it changes with the temperature. The material's absorption coefficient increases with the increase of the temperature. On the other hand, the material's absorption coefficient also changes due to the surface oxidization induced by the temperature rising. The surface appearance mainly refers to the treating status of the tube surface. In order to improve the absorption coefficient, the tube surface is generally coated with graphite or oxide. The different treatments and coats affect greatly the absorption coefficient. Obviously, changes of the material's absorption coefficient are very complex during the forming process. It is very hard to be described accurately. Generally, the change of the absorption coefficient is not considered and it is treated as a constant. The range of the absorption coefficient can be selected as 0.5–0.7 according to the treatment methods in the actual laser tube bending.

2.3 Treatment of the laser spot

In the laser tube bending process simulation, the laser beam is treated as a face flux. The MSC/Marc offers a good interface program. The user subroutine FLUX (F, TS, N, and TIME) can be utilized to define the face heat flux or body heat flux that depends on time, temperature, or position. It can satisfactorily describe the laser heat resource in the laser forming process. Thus, a USER SUBROUTINE FLUX is developed to describe the heat flux density, geometry, dimension, and the scanning velocity numerically. The heating load can be exerted automatically to the relative element faces. Figure 2 gives the flowchart of the user subroutine.

In practical process, the laser spot may be circular or square. The square spot is convenient to deal with although the circular spot is a common shape. The circular spots are usually transferred to the square spots according to the principle of area equality. Thus, the spot size can be described with the dimension of $l \times l$ mm^2. In the laser bending of tubes, the tube absorbs a quantity of heat from the laser beam when the laser beam irradiates the tube surface at a certain velocity. Therefore, the moving laser spot can be simplified as a heating source with the dimension of $l \times l$ mm^2, the scanning velocity v along the surface of the tube and the heat flux density I_m.

The laser beam is Gauss's beam, its heat flux density distribution I is expressed by:

$$I = \frac{2AP}{\pi r_b^2} \exp\left(-\frac{2r^2}{r_b^2}\right) \tag{1}$$

Then, the average heat flux density I_m in the range of the diameter of the laser beam is given by:

$$I_m = \frac{1}{\pi r_b^2} \int_0^{r_b} I(2\pi r_1)\mathrm{d}r_1 = \frac{2\pi}{\pi r_b^2} \int_0^{r_b} \frac{2\mathrm{AP}}{\pi r_b^2} \exp\left(-\frac{2{r_1}^2}{r_b^2}\right) r_1 \mathrm{d}r_1 = \frac{0.865\mathrm{AP}}{\pi r_b^2} \tag{2}$$

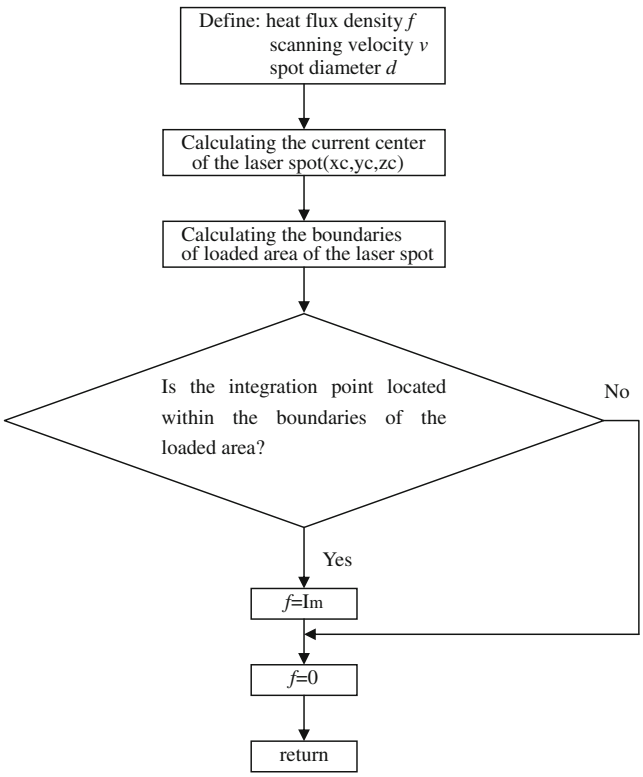

Fig. 2 Flowchart of the user subroutine

where A *is* the absorption coefficient, P is the laser output power, r_b is the radius of the laser beam irradiated to the surface of the tube, and r_1 is the distance between the observed point and the laser beam center. The magnitude of the absorption coefficient is selected as 0.5 in this paper according to the treatment methods in the actual laser tube bending.

2.4 The boundary conditions and initial conditions

The natural cooling-down method is adopted in the paper. In other word, the tube is cooled down naturally in the air. Heat convection and radiation exists between the tube and the surroundings. The convection and radiation boundary conditions are called the third kind of boundary conditions, and can be expressed by:

$$-k\left(\frac{\partial t}{\partial n}\right) = \alpha(T - T_\infty) \tag{3}$$

where k is the heat conductivity, α is the heat exchange coefficient, T is the surface temperature of the sheet metal, and T_∞ indicates the environmental temperature.

The heat exchange coefficient can be written as:

$$\alpha = h + h_r \tag{4}$$

where h is the natural convection exchange coefficient and h_r is the equivalent irradiation exchange coefficient. The natural convection exchange coefficient is determined by Eq. (6) [13].

$$h = 2.15(T - T_\infty)^{0.25} \tag{5}$$

According to irradiation law, the equivalent irradiation exchange coefficient can be expressed as follows

$$h_r = \sigma\varepsilon(T + T_\infty)(T^2 + T_\infty^2) \tag{6}$$

where σ is the Boltzmann constant (5.67×10^{-8} W/m^2 °C), ε is the surface emissivity. Obviously, the equivalent irradiation exchange coefficient is a function of the temperature. The curve of the equivalent irradiation exchange coefficient versus the temperature shown in Fig. 3 can be obtained from Eq. (7). Therefore, the irradiation boundary condition is nonlinear.

The displacements at one end of the tube are restricted, and the other surfaces are displacement free. It is assumed that the tube is initially stress free and strain free. Initial temperature of the tube is 20 °C.

2.5 Material properties

Material properties have a strong influence on the laser-forming process. Because the property parameters are correlative to the temperature, the correlation between

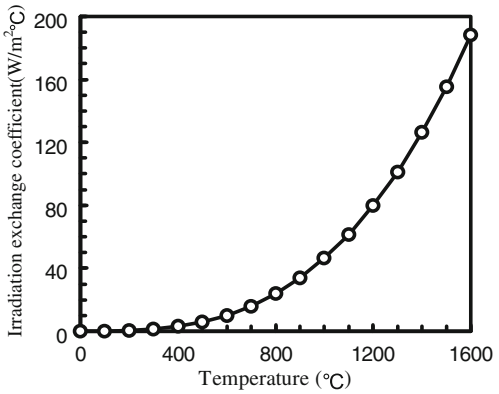

Fig. 3 Variation of equivalent irradiation exchange coefficient with temperature

properties parameters and temperature must be considered in the simulation. The 321 stainless steel tube is used for the study. The material properties variations with the temperatures extract from Reference [14–16].

3 Process simulation of laser tube bending

A specimen of Φ 10×80×1 mm (diameter×length×thickness) is analyzed. Twenty-node brick elements are used. The total element number is 10,400. The finite element mesh is shown in Fig. 4.

The other process parameters are as follows:

Laser output power: P=1 kW
Scanning velocity: v=1.5 m/min
Laser spot diameter: d=5 mm
Initial temperature of sheet metal: T_0=20 °C
Scanning wrap angle: 180°

Based on above technical treatments, a thermomechanical FEM model of the laser tube bending is established. The process of laser tube bending is analyzed numerically. The kinds of fields during the forming process are acquired

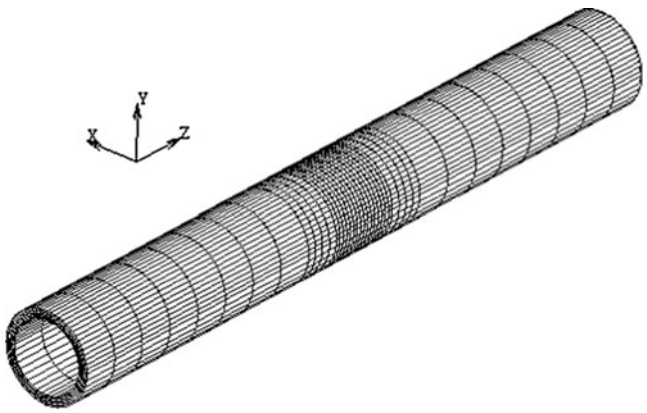

Fig. 4 Finite element model

numerically. It is shown that the tube exhibits relative the forming characteristics going with the laser spot scan.

Figure 5 shows the sketch of the laser scanning process and cross-section of the tube in the heated zone. The central zones of laser scanning side and nonscanning side are selected to study the characteristics of the laser tube bending.

3.1 Single-scan process

Figure 6 shows the variation of temperature with time. The laser spot gets to the zone I at 0.294 s. The irradiation lasts for 0.196 s. The temperature reaches its peak value at 1,099.25 °C at 0.49 s.

Subsequently, the temperature drops down sharply until it reaches to the room temperature. The stress and strain vary with the change of temperature greatly. Figure 7 gives the variation of axial stress with time. At the beginning, the stress state in the zoneIis tensile. When the laser spot irradiates the zone I, the thermal expansion of materials due to temperature rise goes up. But, the surrounding materials restrict the expansion. And then, the stress of zone I become too compressive. At the beginning of the cooling stage, the stress in axial direction recovers from compressive to tensile because of the shrinkage of the material. Subsequently, the tensile stress diminishes gradually. Finally, the stress state is in compressive due to the more shrinkage of material.

Figure 8 shows variations of the thermal strain, total strain, and plastic strain with time. The change of thermal strain is similar to that of temperature. The thermal strain increases from zero to its peak value 0.0143, and then decreases to zero finally. This corresponds with the movement of laser spot. The axial plastic strain is dependent upon the axial stress. At the beginning of the laser irradiation, the material in the heated zone expands due to the temperature rise. When the temperature continues to go up, the axial

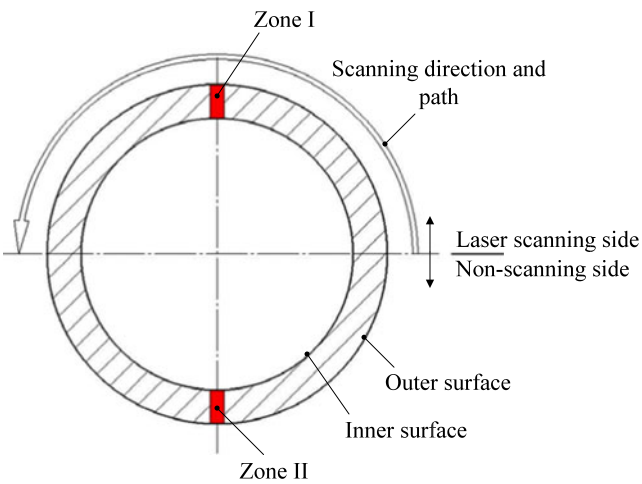

Fig. 5 Sketch of the laser scanning process and cross-section of the tube in the heated zone

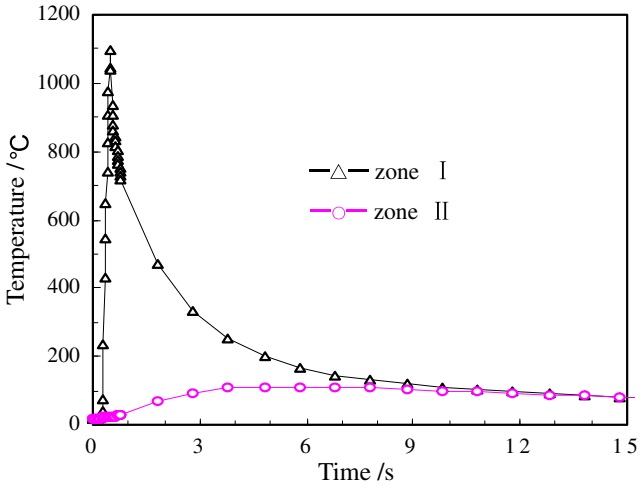

Fig. 6 Variation of temperature with time

stress of in the heated zone becomes too compressive because of the restriction of the surrounding materials. The axial compressive stress rises greatly with the increase of the temperature. In the meanwhile, the yield strength decreases with the temperature rise. The compressive plastic deformation is brought out in the heated zone.

Zone II is not irradiated directly by laser beam. The temperature rises slowly due to the heat conduction (shown in Fig. 6). The temperature reaches its peak value at 111.64 °C at 5.80 s. A great gradient occurs between the laser scanning side and the nonscanning side. At the beginning, the stress state in zone II is compressive. The stress of zone I become too tensile with the development of the temperature. The stress keeps a lower value all the time. Thus, the plastic deformation in zone II is not induced.

Obviously, the gradient and development of the temperature between the laser scanning side and the nonscanning side leads to the changing complexity of the stress and strain. The

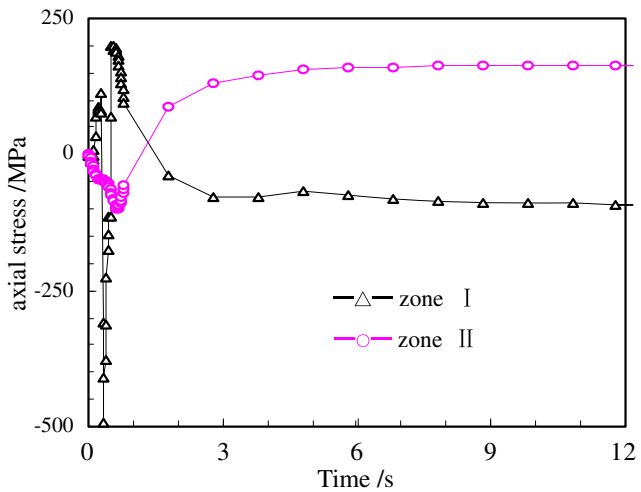

Fig. 7 Variation of axial stress with time

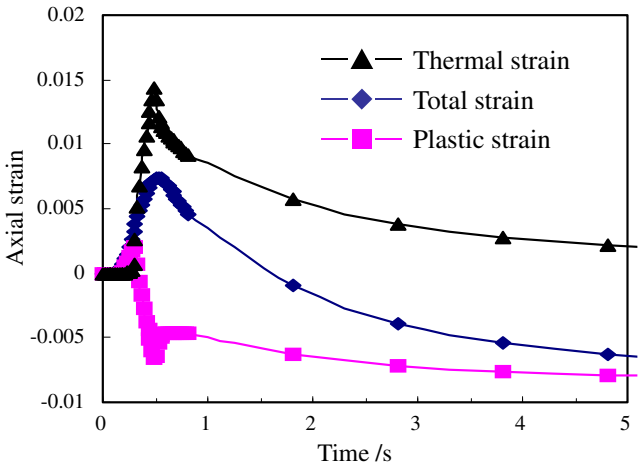

Fig. 8 Variation of the axial strain with time

final strain of the laser scanning side resulting by the shrinkage of the heated zone is −0.0084 in axial direction. The length of the laser scanning side becomes shorter than that of nonscanning side after cooling. The length difference between both sides makes the tube produce the bending angle.

Figure 9 gives the variation of the displacement of the free end in *y* direction with the time. At the beginning of the laser scanning, the displacement of the free end in *y* direction is negative. The largest displacement is −0.1519 mm. It is obvious that the tube produces reverse bending deformation. But the sustaining time of the reverse bending is very short. The reverse bending deformation reduces gradually with the successive laser scanning. Finally, the displacement of the free end in *y* direction remains constant, that is 0.1772 mm. This is similar to the laser bending of sheet metals.

3.2 Multiscan process

A bending angle acquired in a scan is small. In order to obtain the desired bending angle in practical engineering, the tube has to be scanned repeatedly along the same scanning path. Figure 10 gives the variation of the axial plastic strain of the

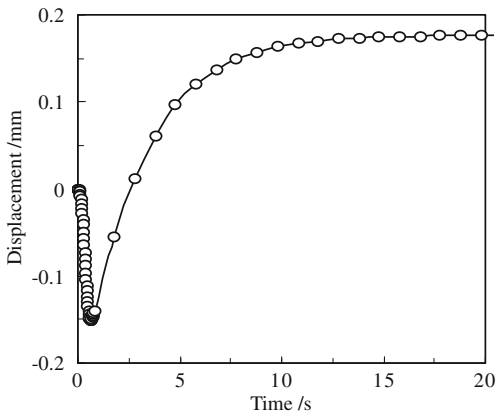

Fig. 9 Variation of displacement in the *Y* direction with time

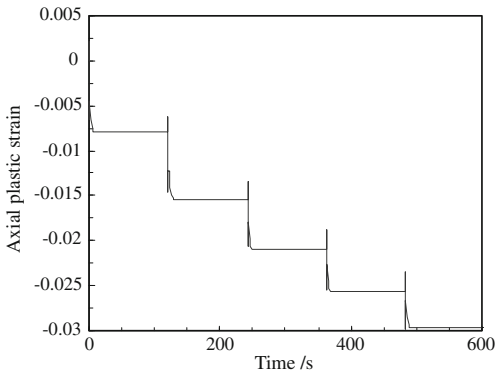

Fig. 10 Variation of axial plastic strain in zone I with time

irradiated side with time. The axial plastic strain of the irradiated zone becomes larger and larger with the increase of the number of scans. Meanwhile, the axial plastic strain of the non-irradiated side is almost zero. The different step of the axial plastic strain difference is generated between two successive scans. Thus, the axial plastic strain difference between the irradiated side and non-irradiated side augments in the multiscan laser bending process. Consequently, the bending angle of the tube increases.

Figure 11 gives the influence of the number of scans on bending angle, it is seen that the relationship between the number of scans and the bending angle keeps linear. The bending angle acquired in the first scan is largest. In the course of the first scan, the whole heated zone happens to shrink during the cooling stage, the difference between shrinkages of the upper surface and lower surface makes the tube generate the bending deformation. When the tube continues to be irradiated repeatedly, the shrinking result during the cooling stage is less than that in the first irradiation. The bending angle obtained in subsequent irradiation is smaller than that in the first irradiation. The interval between two successive scans is short. The successive scan begins before the sheet cools completely. Seen from Fig. 12, the temperature peak of the heated zone in the successive scan is a little higher than that in the last time. It should be helpful to plastic deformation that the material's yield

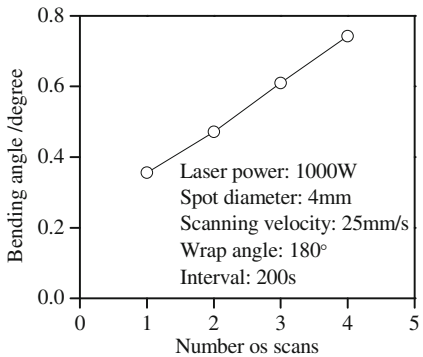

Fig. 11 Variation of bending angle with scanning number

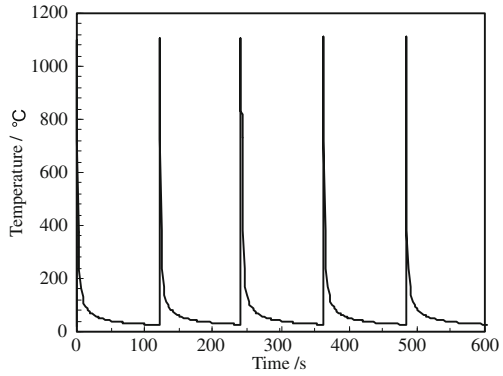

Fig. 12 Variation of temperature in zone I with time

strength drops down because of the higher temperature in the heated zone, but the plastic strain difference between two continuous scans becomes smaller and smaller. The step generated between two successive scans is also lower and lower. The ability that the successive scans induce the axial plastic strain decreases. Figure 13 gives the variation of displacement in *y* direction with time. It is indicated clearly that there are distinct differences among different irradiating process. The contribution of the first scan to the tube deformation is largest, and contributions of successive scans to the tube deformation decrease gradually.

4 Process optimization of laser tube bending

In order to reduce the time consumption, a 321 stainless steel tube specimen with Φ 5×24×0.5 mm (diameter× length×thickness) is analyzed.

4.1 Establishment of process optimization model

4.1.1 Design variable

Although there are many factors that influence the laser bending of tubes, such as forming process parameters, geometric parameters, and material property parameters,

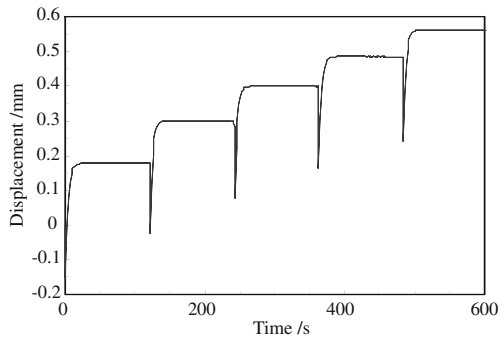

Fig. 13 Variation of displacement in zone I in *Y* direction with time

Table 1 Limits of design variables

Design variables	Lower limit	Upper limit
laser power (W)	100	1200
laser beam diameter (mm)	1	10
laser scanning velocity (mm/s)	10	35
Scanning wrap angle (°)	0	180

geometric and material's property parameters are constant for a definite forming process. The main variable factors are forming process parameters, including laser power *P*, scanning velocity *v*, spot diameter *d*, and wrap angle ψ, which are determinative factors for laser tube bending. Thus, during process optimization, laser power, beam diameter, and scanning velocity are regarded as the design variables. The design variable vector can be written as,

$$\mathbf{X} = [P, v, d, \psi] \tag{7}$$

The limits of design variables are determined by capability of laser machine and process requirements. According to

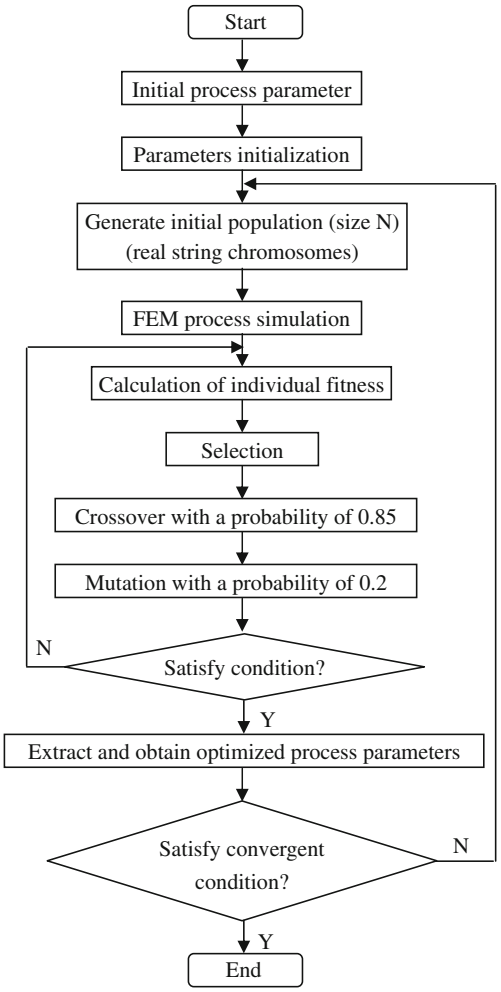

Fig. 14 Optimization system flowchart

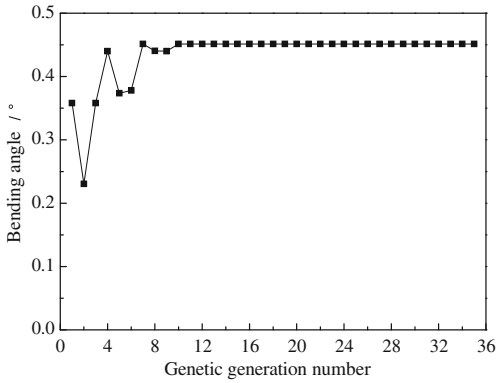

Fig. 15 Variation of the objection function with genetic generation number

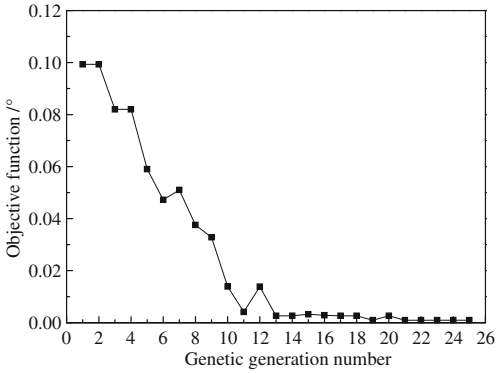

Fig. 16 Variation of the objection function with genetic generation number

requirements of the laser tube bending process, the limits of the design variables are listed in Table 1.

4.1.2 Objective function

During laser tube bending, the principal process requirement is to obtain the desired bending angle. Meanwhile, the process must be reasonable on the basis of satisfying the forming precision and efficiency. Aiming at different process requirements, there are different objective functions.

Maximum angle bending In order to improve the forming efficiency, the maximum bending angle after single laser scan can be approached by means of matching process parameters. The precondition of the process optimization is the microstructure of the material cannot be destroyed. Thus, the optimization model of the laser bending process is

$$\max f = \alpha(p, d, v, \psi) \tag{8}$$

where, α is bending angle corresponding to a set of design variables.

Fixed angle bending Generally, the desired bending angle is decided during laser tube bending. Therefore, the fixed bending angle after single laser scan can be approached by means of matching process parameters. The optimization model of the fixed angle bending is

$$\min f = |\alpha(p, d, v, \psi) - \beta| \tag{9}$$

where, β is the desired bending angle, α is bending angle corresponding to a set of design variables. When the objective function approaches zero, the bending angle approaches the desired bending angle β.

4.1.3 Constraint condition

The precondition of the process optimization is the microstructure of the material cannot be destroyed. Thus, the constraint condition of the laser tube bending is

$$T_p < T_1 \tag{10}$$

where T_p is the peak temperature during laser tube bending and T_1 is constraint temperature which is less than the material's melting point in order to avoid the microstructure of the material being destroyed. In our work, the studied material is the 321 stainless steel tube. Its melting point is 1,350 °C. The constraint temperature T_1 is defined as 1,300 °C.

4.2 Establishment of process optimization system

Both objective functions include the item $\alpha(p, d, v,$ and $\psi)$. At present, analytical formulas of the laser tube bending are not perfect, presented analytical formulas cannot satisfy the demand of process optimization.

Genetic algorithms [17, 18] is a random search method of solving optimization problems by imitating the evolutionary process based on the mechanics of Darwin's natural selection. During optimization, genetic algorithms only need objective function value and do not need derivative information. Thus, theoretically speaking, genetic algorithms may apply to any optimization problem as long as the objective function value can be obtained.

Table 2 Optimized process parameters

Laser power (W)	Scanning velocity (mm/s)	Spot diameter (mm)	Wrap angle (°)
381.24	16.34	3.37	123.1

Table 3 Optimized process parameters of the fixed angle bending

Laser power (W)	Scanning velocity (mm/s)	Spot diameter (mm)
426.12	14.31	4.9

The finite element method has become a powerful tool to analyze the laser tube bending process. Thus, the commercial finite element analysis software, such as MSC/Marc, Ansys, and Abaqus, can be used as solvers during optimization based on genetic algorithms. The process optimization system includes two independent modules. They are genetic algorithms module and FEM process simulation module. In our study, FEM process simulation solver is MSC/Marc. Figure 14 gives the optimization system flow chart.

4.3 Optimization results

4.3.1 Process optimization of the maximum angle bending

Figure 15 gives variation of the objective function value (bending angles) with genetic generations. Obviously, the objective function rapidly approach to maximum with the increase of the genetic generation number. When the genetic generation number is over 12, the objective function keeps constant. It is 0.4514°. The bending angle corresponding to the initial process parameters is 0.2008°. The increasing amplitude of optimized bending angle is 124.8 %. Table 2 gives optimized process parameters of the maximum angle bending.

4.3.2 Process optimization of fixed angle bending

During process optimization of fixed angle bending, the desired bending angle is 0.3°, namely β=0.3° in Eq. (3). The scanning wrap angle is constant, and it is 180°.

Figure 16 gives variation of the objective function with genetic generations during process optimization of the fixed angle bending. When the iterative number is 15, the objective function is 9.4×10^{-4}°. The corresponding bending angle is 0.30094°. The error comparing with the desired bending angle 0.3° is 0.31 %. Meanwhile, the peak temperature is 1,226 °C. Table 3 gives optimized process parameters of the fixed angle bending.

The finite element simulation is integrated with the genetic algorithm. Process optimizations of maximum angle bending and fixed angle bending after single laser scan are realized. Based on process optimizations, the optimum match of process parameters can be obtained. Previous work is only limited to finite element analysis, analytical analysis and experiments, and is unable to obtain the optimum process parameters.

5 Conclusions

1. The gradient and development of the temperature between the laser scanning side and the nonscanning side leads to the changing complexity of the stress and strain. Consequently, the length of the laser scanning side becomes shorter than that of nonscanning side after cooling. The length difference between both sides makes the tube produce the bending angle. The relationship between the number of scans and the bending angle is about in direct ratio. The bending angle induced by the first irradiated time is largest.
2. In our study on laser bending of 321 stainless steel tube with dimensions Φ 5×24×0.5 mm (diameter×length×thickness), the maximum bending angle can be reached when the laser power, spot diameter, scanning velocity, and scanning wrap angle are 381.24 W, 3.37 mm, 16.34 mm/s, and 123.1°, respectively. When the laser power, spot diameter, and scanning velocity are 426.12 W, 4.9 mm, 14.31 mm/s, respectively, a fixed angle bending 0.3° can be achieved.

Acknowledgments The research work was supported by the Program for New Century Excellent Talents in University (NCET-08-0337), and Program for Changjiang Scholars and Innovative Research Team in University of Ministry of Education of China under grant no IRT0931.

References

1. Geiger M, Vollertsen F (1993) The mechanism of laser forming. CIRP Ann 42:301–304
2. Arnet H, Vollertsen F (1995) Extending laser bending for the generation of convex shapes. J Eng Math 209:433–442
3. Yang L, Wang M, Wang Y, Chen Y (2010) Dynamic analysis on laser forming of square metal sheet to spherical dome. Int J Adv Manuf Technol 51:519–539
4. Xia M, Yan Q, Zuo D, Xie J (2011) An investigation on multistage bending of blank sheet into cylindrical tube by experiment and numerical simulation. Int J Adv Manuf Technol 53:145–155
5. Hao N, Li L (2003) Finite element analysis of laser tube bending. Appl Surf Sci 208–209:437–441
6. Hao N, Li L (2003) An analytical model for laser tube bending. Appl Surf Sci 208–209:432–436
7. Hsieh H, Lin J (2005) Study of the buckling mechanism in laser tube forming. Opt Laser Technol 37:402–409
8. Hsieh H, Lin J (2005) Study of the buckling mechanism in laser tube forming with axial preloads. Int J Mach Tool Manuf 45:1368–1374
9. Zhang J, Cheng P, Zhang W, Graham M, Jones J, Jones M, Lawrence Yao Y (2006) Effects of scanning schemes on laser tube bending. J Manuf Sci E-T ASME 128:20–33
10. Safdar S, Li L, Sheikh MA, Zhu L (2007) Finite element simulation of laser tube bending: Effect of scanning schemes on bending angle, distortions and stress distribution. Opt Laser Technol 39:1101–1110
11. Guglielmotti A, Quadrini F, Squeo EA, Tagliaferri V (2008) Diode laser forming of stainless steel tubes. Int J Mater Form (SUPPL.1): 1343–1346
12. Vollertsen F, Holzer S (1995) 3D-thermomechanical simulation of laser forming, simulation of materials processing: theory, methods and applications. In: Dawson PR (ed) SF Shen. Balkema, Rotterdam, pp 785–791

13. Xie H, Xu X, Liu X, Wang G (2005) Numerical simulation on hot strip temperature field in laminar cooling process. J Iron Steel Res 17:33–35,50 (in Chinese)
14. Davis JR (1990) Metals handbook Vol.1. ASM International Ohio
15. Davis JR (1990) Metals handbook Vol.2. ASM International Ohio
16. Tan Z, Guo G (1994) Thermal-physical properties of alloys (in Chinese). Metallurgical Industry Press, Beijing
17. Mitsuo G, Runwei C (2000) Genetic algorithms and engineering optimization. Wiley, New York
18. Lihong Q, Shengping L (2012) An improved genetic algorithm for integrated process planning and scheduling. Int J Adv Manuf Technol 58:727–740